Materials Science in Semiconductor Processing 26 (2014) 162–168

Contents lists available at ScienceDirect

Materials Science in Semiconductor Processing

journal homepage: www.elsevier.com/locate/mssp

Single wall carbon nanotube/titania nanocomposite photoanodes enhance the photovoltaic performance of cadmium selenide quantum dot-sensitized solar cells

Ali Badawi [a,*], N. Al-Hosiny [a,b], S. Abdallah [a,c], Amar Merazga [a], H. Talaat [d]

[a] Department of Physics, Faculty of Science, Taif University, Taif, Saudi Arabia
[b] Department of Physics, Faculty of Science, Aljouf University, Saudi Arabia
[c] Department of Mathematical and Physical Engineering, Faculty of Engineering (Shoubra), Benha University, Cairo, Egypt
[d] Physics Department, Faculty of Science, Ain Shams University, Abbassia Cairo, Egypt

ARTICLE INFO

Available online 13 May 2014

Keywords:
SWCNTs/TiO_2 nanocomposite photoanode
CdSe quantum dot
Direct adsorption
Quantum dots sensitized solar cell
Photovoltaic cells

ABSTRACT

Improving the photovoltaic performance of CdSe quantum dots sensitized solar cells (QDSSCs) using 0.2 wt% of single walled carbon nanotubes/Titania (SWCNTs/TiO_2) nanocomposite photoanode is reported. These SWCNTs/TiO_2 nanocomposite films were prepared by mechanical mixing and spread on the photoanode by a doctor blade method. The current density–voltage (J–V) characteristic curves of such assembled QDSSCs were measured at AM 1.5 simulated sunlight. Solar cells based on SWCNTs/TiO_2 nanocomposite photoanode achieves 58% increase in power conversion efficiency (η) compared with those based on plain TiO_2 NPs photoanode under a AM 1.5 simulated sunlight and for dipping time of 6 h. The significant improvement of J_{sc} and η for CdSe QDSSCs based on SWCNTs/TiO_2 nanocomposite photoanode is due to the enhancement in the absorption of the incident light and rapid electron transport through the SWCNTs compared to the plain TiO_2 NPs. Furthermore, the linear increase in J_{sc} with increasing intensity of the sunlight indicates the sensitivity of the assembled cells.

1. Introduction

Throughout the last decade, science has made great strides towards improving the performance of quantum dots sensitized solar cells (QDSSCs) [1–5]. In this type of solar cell, quantum dots (QDs) are adsorbed onto large band gap metal oxides nanoparticles (NPs) such as TiO_2 [6,7], ZnO [7,8], or SnO_2 [7] to act as sensitizers. Among the parameters that make QDs attractive candidates are the ability of tuning the band gap of these QDs through size control to match the sunlight spectra [2,9,10], high extinction coefficients due to quantum confinement effects [6,11], unique electronic and optical properties, large intrinsic dipole moments that lead to rapid charge separation [12], and intrinsically strong light absorbers [13]. Furthermore, QDSSCs have larger surface areas and provide a technically and economically credible alternative to conventional cells, such as silicon photovoltaic or dye-sensitized solar cells (DSSCs). DSSCs have many limitations, such as difficulties in utilizing the infrared region of the solar spectrum and instability over long periods of time. Several research efforts have already been carried out using the following QDs as photosensitizers: CdS [14,15], CdSe [10,16–18], CdTe [2,19], PbSe [20], PbS [21,22], InAs [23], ZnSe [24], and Ag_2Se [25]. Cadmium chalcogenides (CdX; X=S, Se, and Te) QDs are relatively simple to synthesize, and easy to control their sizes to harvest as much light energy, especially in the visible region of the solar spectrum. These characteristics make CdX QDs appropriate sensitizers for making QDSSCs

* Corresponding author. Tel.: +966 543414808; fax: +966 27241880.
E-mail address: adaraghmeh@yahoo.com (A. Badawi).

http://dx.doi.org/10.1016/j.mssp.2014.04.028
1369-8001/

[26]. According to previous studies [2,10,14,17] related to tuning photocurrent response through size control of CdX QDSSCs, CdSe QD of 4.52 nm in size (corresponding to 542 nm absorption edge) is the optimal CdX QD size for photovoltaic applications.

To deposit QDs onto large band gap metal oxides, mainly, two different strategies are used [27]: in situ growth of QDs by either a chemical bath deposition (CBD) containing both cationic and anionic precursors [6] or the successive ionic layer adsorption and reaction deposition (SILAR) method [10]. These methods provide good surface coverage, but they limit the control of QD size and yield a broad size distribution [9]. These drawbacks can be avoided if the QDs are synthesized prior (ex situ) to being deposited [28] via electrophoretic deposition (EPD) [9], linker-assisted adsorption (LA) [29], or direct adsorption (DA) [5,18,30] using different dipping times. This last method was the one applied in this work.

Single walled carbon nanotubes (SWCNTs) possess many attractive properties, such as large surface area, low-cost, light weight, high electrical conductivity, excellent mechanical strength, three-dimensional flexibility and outstanding electrocatalytic property [31–33]. Carbon nanotubes (CNTs) based composites have received considerable attention due to the fact that the composite conductivity can be increased significantly with a relatively low concentration of CNTs in the host material [34,35]. CNTs can increase the UV light absorption and enhance electron transport in composite films [36]. Many studies [31,32,37–39] showed that CNTs can significantly improve the short circuit current density (J_{sc}) and power conversion efficiency (η) of dye-sensitized solar cells (DSSCs). Peining et al. [40] and Yu et al. [41] have shown that 0.2 wt% of CNTs is the optimum concentration in the TiO_2 matrix for best photovoltaic performance in DSSCs.

In this work, we synthesized CdSe QDs with a certain size (4.5 ± 0.1 nm) to be used as a sensitizer in QDSSCs using a chemical deposition (CD) technique. These colloidal QDs were adsorbed onto 0.2 wt% of SWCNTs/TiO_2 nanocomposite photoanode using the DA technique under ambient conditions. The effect of SWCNTs on the photovoltaic parameters (J_{sc}, open circuit voltage (V_{oc}), fill factor (FF), and η) of CdSe QDSSCs incorporated by SWCNTs/TiO_2 nanocomposite photoanode was studied. However, to the best of our knowledge, this is the first time that the photovoltaic performance of CdSe QDSSCs using SWCNTs/TiO_2 nanocomposite photoanode is reported. Furthermore, the *J–V* characteristic curve of CdSe QDSSCs at various illumination intensities was also measured.

2. Experiment

2.1. Synthesis of CdSe QDs

Colloidal CdSe QDs were synthesized using the method of Talapin et al. [42]. We used hexadecylamine (HDA) as a capping agent, together with trioctylphosphine oxide (TOPO) to facilitate the preparation of highly monodispersed nanocrystals (size distribution $\leq 5\%$). The sample was immediately cooled and diluted with toluene.

2.2. Preparation of QDSSC electrodes

A colloidal paste of TiO_2 NPs was prepared using the method of Syrrokostas et al. [43] as follows: 3 g of commercial Degussa P25 TiO_2 nanopowders (P25) (Degussa AG, Dusseldorf, Germany) was ground in a porcelain mortar and pestle and mixed with 1 mL of distilled water containing acetyl acetone (10% v/v). Acetyl acetone was used as a dispersing agent because it prevents the coagulation of TiO_2 NPs and affects the porosity of the film. The paste was diluted further by the slow addition of distilled water (4 mL) under continued grinding. The addition of water controls the viscosity and final concentration of the paste. Finally, a few drops of a detergent (Triton X-100) was added, reducing the surface tension of the paste, to facilitate even spreading and reducing the formation of surface cracks. To synthesize 0.2 wt% of SWCNTs/TiO_2 nanocomposite paste, the method of Yu et al. [41] was followed. Briefly, SWCNTs (diameter $\sim$2 nm and length$\sim$30 μm purchased from Chengdu Organic Chemicals Co. Ltd.) were rinsed with deionized water three times and dried at 60 °C under ambient conditions. Then 0.006 g of SWCNTs was added to the previous TiO_2 NPs paste and dispersed using an ultrasonic horn for 30 min. After stirring for 2 h, the 0.2 wt% SWCNTs/TiO_2 nanocomposite paste was coated on FTO substrate using the doctor blade technique on a transparent conducting glass substrate made from SnO_2:F (FTO) (purchased from Solaronix, TCO22-7) with a sheet resistance of 7 Ω/sq and $>$80% transmittance in the visible region. Then, the films were sintered at 450 °C for 1 h. After cooling to room temperature, the SWCNTs/TiO_2 nanocomposite photoanodes were immersed into a colloidal CdSe QDs solution for four different times (1, 3, 6, and 24 h), and kept at room temperature. After solvent evaporation, the final nanocomposite film thickness was 8 ± 1 μm as measured by a profilometer (Alpha step, Tencor). The counter electrodes were FTO substrate sheets coated with Pt.

2.3. Assembly of CdSe QDSSC

The working photoanode and Pt counter electrode were assembled into a sandwich type cell using clamps. Both electrodes were sealed using a hot-melt polymer sheet (Solaronix, SX1170-25PF) that was 25 μm thick to avoid evaporation of the electrolyte. The active area of the assembled cells was 1 cm × 1 cm. Finally, an iodide electrolyte solution was prepared by dissolving 0.127 g of 0.05 M iodine (I_2) in 10 mL of water-free ethylene glycol and then adding 0.83 g of 0.5 M potassium iodide (KI). The electrolyte was inserted into the cell with a syringe, filling the space between the two electrodes.

2.4. Measurements

The absorption spectra of the CdSe QDs (before and after adsorption on SWCNTs/TiO_2 nanocomposite photoanodes) were recorded using a UV–vis spectrophotometer (JASCO V-670). In addition, the size of the QDs was measured by a high resolution transmission electron microscope (HRTEM). The current density–voltage (*J–V*) characteristics were recorded with a Keithley 2400 voltage

source/ammeter using Green Mountain IV-Sat 3.1 software, while the CdSe QDSSCs were subjected to a solar simulator illuminator (ABET technologies, Sun 2000 Solar Simulators, USA) operating at 100 mW/cm^2 (AM1.5G). The intensity of the incident solar illumination was adjusted to 1 sun condition using a Leybold certified silicon reference solar cell (Model: 57863) Solar cell 2 V/0.3 A STE 4/100). The *J–V* characteristic curves of CdSe QDSSCs at various illumination intensities were studied and all experiments were carried out under ambient conditions.

3. Results and discussion

3.1. Characterization of CdSe QDs

The average particle size of the prepared CdSe QDs was found to be 4.5 ± 0.1 nm using HRTEM. Fig. 1(a) and (b) shows the HRTEM micrograph and a histogram of particle size distribution for CdSe QDs respectively.

The UV–vis absorption spectrum of CdSe QDs in a colloidal solution was recorded and shown in Fig. 2. The first excitonic absorption edge is easily observed at 542 nm which corresponds to 2.26 eV energy band gap. The blue-shift with respect to bulk CdSe (1.74 eV [44]) is due to the quantum confinement effect.

The corresponding CdSe QD size was also calculated using the following effective mass approximation (EMA) model [45]:

$$E_{g(Nano)}(R) = E_{g(bulk)} + \frac{h^2}{8R^2}\left[\frac{1}{m_e} + \frac{1}{m_h}\right] - \frac{1.8e^2}{4\pi\varepsilon\varepsilon_0 R} \quad (1)$$

where m_e ($0.13m_0$) and m_h ($0.45m_0$) [44,46] are the effective masses of the electron and hole, respectively, m_0 is the electron mass, $E_{g(bulk)}$ (1.74 eV) is the bulk crystal band gap, R is the average radius of the nanocrystal, $E_{g(Nano)}$ is the QD band gap value, h is Planck's constant and ε (5.8) [44] is the relative permittivity. The calculated average radius of the CdSe QDs based on Eq. (1) is 4.52 nm, which is comparable to that obtained by HRTEM micrograph.

3.2. Structural properties of SWCNTs/TiO_2 nanocomposite photoanode

Fig. 3 shows X-ray diffraction (XRD) patterns for both TiO_2 NPs/FTO and 0.2 wt% SWCNTs/TiO_2 nanocomposite films/FTO and the inset in the figure shows the XRD

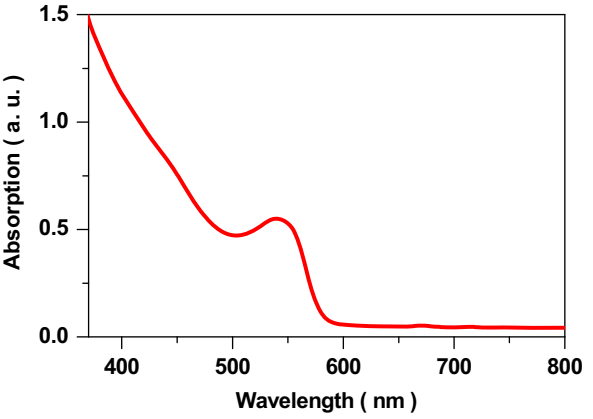

Fig. 2. UV–vis absorption spectra for CdSe QDs.

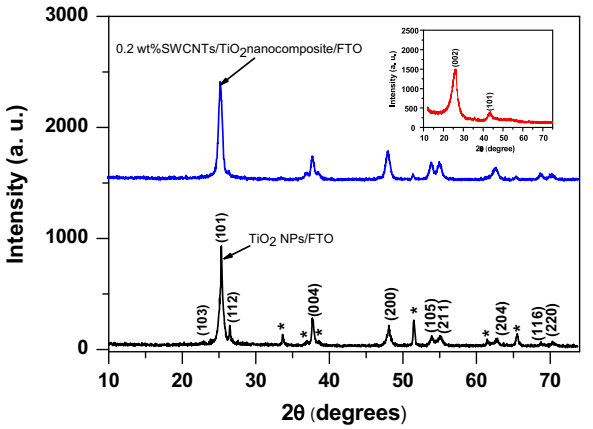

Fig. 3. XRD patterns of TiO_2 NPs/FTO film, and 0.2 wt% of SWCNTs/TiO_2 nanocomposite film on FTO. Inset shows the XRD pattern for SWCNTs.

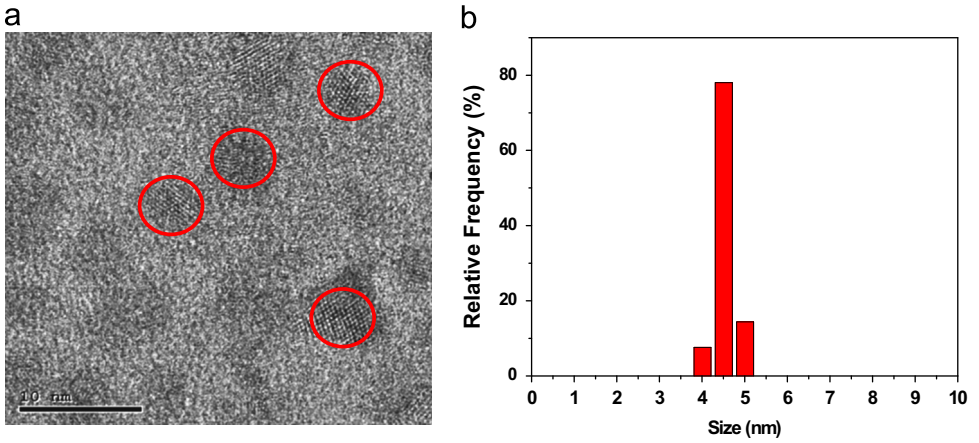

Fig. 1. (a) HRTEM micrograph for CdSe QDs and (b) the histogram of particle size distribution.

pattern for SWCNTs. It is clearly seen that the crystalline phases of anatase TiO_2 NPs are found in the TiO_2/FTO film, in addition to SnO_2:F (FTO) phases (denoted by ∗ in Fig. 3). The peaks at 25.30°, 37.03° 37.76°, 48.07°, 53.92° and 62.82° corresponding to the (101), (103), (004), (200), (105), and (204) planes of anatase TiO_2 respectively (Joint Committee on Powder Diffraction Standards (JCPDS Card no. 21-1272) [47] are indicated. Also, the diffraction pattern of SWCNTs/TiO_2 nanocomposite film is similar to that of TiO_2 NPs/FTO film. However, the characteristic peak of SWCNTs at $2\theta = 26.6°$ is not observed in the XRD patterns of the nanocomposite. The disappearance of SWCNTs characteristic peaks in the XRD patterns of SWCNTs/TiO_2 nanocomposite film may be due to the homogeneous dispersion of SWCNTs in TiO_2 NPs paste, the absence of SWCNTs aggregation in the nanocomposite paste, the small mass ratio (0.2 wt%) of SWCNTs compared with plain TiO_2, and the high crystallinity of TiO_2 NPs.

3.3. Characterization of CdSe QD sensitized SWCNTs/TiO_2 nanocomposite photoanode (the working photoanode)

Fig. 4 shows the UV–vis absorption spectra of CdSe QD sensitized SWCNTs/TiO_2 nanocomposite photoanodes for various dipping times (0,1, 3, 6, and 24 h) as indicated. It is clearly seen that the absorption is enhanced as the adsorption time increases, due to large amount of CdSe QD loading. Also in the visible region, the difference between 6 and 24 h of dipping is not noticeable. This may be due to saturation effect.

To ensure that the adsorption of CdSe QDs onto the TiO_2 SWCNTs/TiO_2 nanocomposite photoanodes takes place, EDX was performed for it. The results are shown in Fig. 5 where the peaks of CdSe, and C as well as Ti and O_2 are indicated.

Moreover, the UV–vis absorption spectra of plain TiO_2 NPs photoanode, CdSe QDs sensitized plain TiO_2 NPs photoanode, SWCNTs/TiO_2 nanocomposite photoanode and CdSe QDs sensitized SWCNTs/TiO_2 nanocomposite photoanode are recorded and shown in Fig. 6. It is clearly

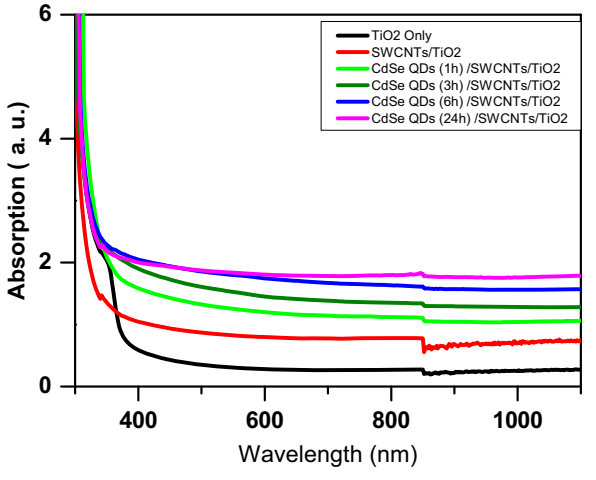

Fig. 4. UV–vis absorption spectra of CdSe QDs SWCNTs/TiO_2 nanocomposite photoanode at different times of dipping as indicated.

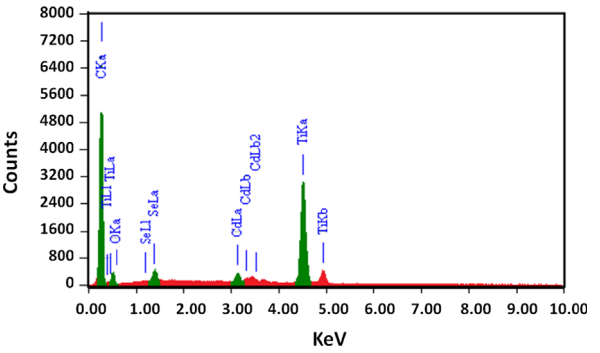

Fig. 5. EDX of CdSe QDs adsorbed onto SWCNTs/TiO_2 nanocomposite photoanodes.

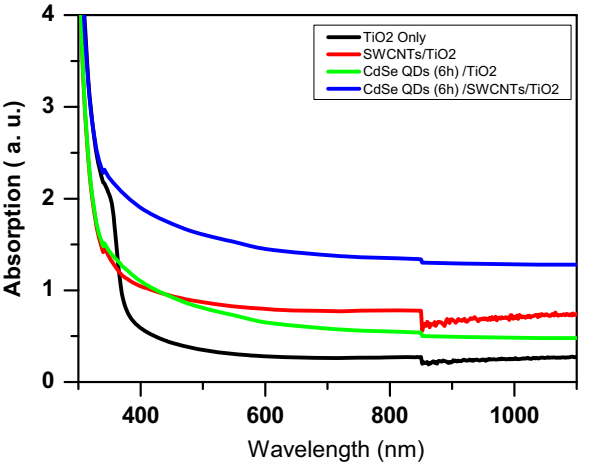

Fig. 6. UV–vis absorption spectra of plain TiO_2 photoanode, SWCNTs/TiO_2 nanocomposite photoanode, CdSe QDs/TiO_2 NPs photoanode, and CdSe QDs SWCNTs/TiO_2 nanocomposite photoanode for 6 h dipping time.

evident that the absorption of CdSe QDs sensitized SWCNTs/TiO_2 nanocomposite photoanode is higher than that of CdSe QDs sensitized plain TiO_2 NPs photoanode. This behavior indicates that more CdSe QDs have been adsorbed on the SWCNTs/TiO_2 nanocomposite photoanode. Such an increase in the amount of CdSe QDs is due to high roughness and porous surface of SWCNTs/TiO_2 nanocomposite [48].

3.4. Photovoltaic performance of CdSe QDSSCs using SWCNTs/TiO_2 nanocomposite photoanode

The photocurrent density–voltage (J–V) characteristics were used to investigate the effect of the dipping times (1, 3, 6, and 24 h) on the photovoltaic performance of CdSe QDSSCs based on SWCNTs/TiO_2 nanocomposite photoanode. The J–V characteristics curves measured under simulated sunlight with an intensity of 100 mW/cm^2 (AM 1.5G) are shown in Fig. 7. The photovoltaic characteristics parameters (V_{oc}, J_{sc}, FF, and η) for CdSe QDSSCs are given in Table 1. It is observed that both J_{sc} and η increase as the dipping time increases up to 24 h. This result could be explained in terms of the dipping time: as it increases up to 24 h, additional amount of CdSe QDs is loaded because

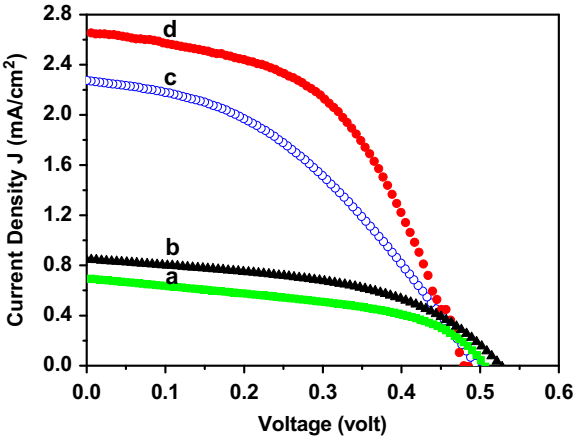

Fig. 7. *J –V* characteristics curves of CdSe QDSSCs using SWCNTs/TiO_2 nanocomposite photoanode for (a) 1 h, (b) 3 h, (c) 6 h, and (d) 24 h dipping time.

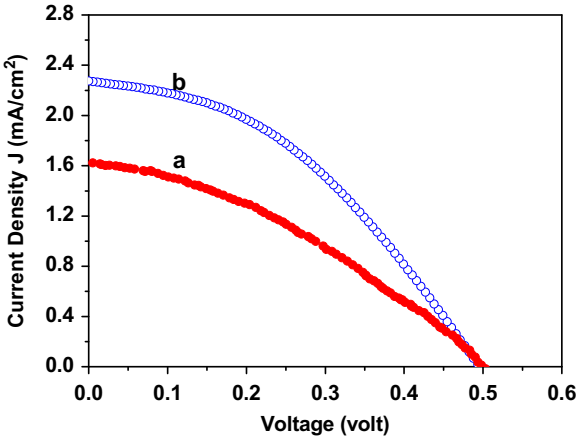

Fig. 8. *J–V* characteristics curves of CdSe QDSSCs using (a) plain TiO_2 NPs photoanode and (b) SWCNTs/TiO_2 nanocomposite photoanode for 6 h dipping time.

Table 1
J–V characteristic parameters of CdSe QDSSCs using SWCNTs/TiO_2 nanocomposite photoanodes at different dipping times.

Dipping time (h)	$V_{oc} \pm 0.02$ (V)	$J_{sc} \pm 0.01$ (mA/cm^2)	FF	η (± 0.01) %
1	0.50	0.69	0.49	0.17
3	0.51	0.87	0.48	0.21
6	0.49	2.27	0.41	0.46
24	0.48	2.65	0.50	0.64

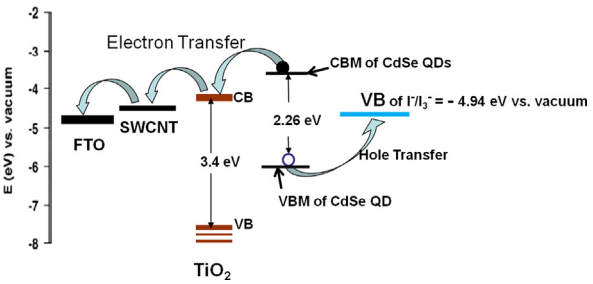

Fig. 9. Schematic energy levels diagram of CdSe QDs, TiO_2, SWCNT, and FTO.

of high roughness and porous surface of SWCNTs/TiO_2 nanocomposite [48].

It is observed from the table that for a dipping time of 6 h, CdSe QDSSCs based on SWCNTs/TiO_2 nanocomposite photoanode give J_{sc}=2.27 mA/cm^2 and η=0.46%, which shows a remarkable increase in both parameters from our previous study [17], using CdSe QDSSCs based on TiO_2 NPs photoanode. In that study the values of J_{sc} and η were 1.62 mA/cm^2 and 0.29% respectively. Fig. 8 shows the *J–V* characteristics curves of CdSe QDSSCs based on plain TiO_2 NPs photoanode and on SWCNTs/TiO_2 nanocomposite photoanode respectively for the 6 h dipping time. This significant improvement of about 40% in J_{sc} and 58% increase in η for CdSe QDSSCs based on SWCNTs/TiO_2 nanocomposite photoanode, with V_{oc} remaining constant (0.50 ± 0.02 eV), is mainly attributed to three factors. First, the improvement in the absorption of the nanocomposite films is due to the roughness surface structure of SWCNTs/TiO_2 nanocomposite film [48], which leads to increased loading of CdSe QDs on the film. Second, the rapid electron transport through the SWCNTs, offering fast interpaths due to the superior electrical conductivity of SWCNTs ($10^2\ \Omega^{-1}\ m^{-1}$ [49]) compared to the TiO_2 NPs ($\sim 8.11 \times 10^{-9}\ \Omega^{-1}\ m^{-1}$ [50]). Third, the DA technique, used to deposit CdSe QDs onto SWCNTs/TiO_2 nanocomposite film, leads to pin the CdSe QDs bands to that of TiO_2 NPs without any barriers, which results in a direct electronic interaction between the two semiconductor materials (CdSe QDs and TiO_2 NPs). So, DA technique minimizes the electrons injection time from the conduction band minimum of CdSe QDs to that of TiO_2 NPs an then to SWCNTs. Fig. 9 shows stepwise energy levels of CdSe QDs, TiO_2, SWCNT, and FTO. Such energy levels are beneficial for electrons to transport from the conduction band of CdSe QDs to FTO glass SWCNTs/TiO_2 nanocomposite. Our results are in good agreement with others [40,41]. Peining et al. [40] fabricated a DSSCs using TiO_2 coated CNTs (TiO_2–CNTs). In their work, they concluded that TiO_2–CNTs content (0.2 wt%) cell showed $\sim$50% increase in η. They attributed this enhancement mainly to the increase in J_{sc} due to improvement in interconnectivity between the TiO_2 particles and the TiO_2–CNTs in the porous TiO_2 film.

The photovoltaic performance of the assembled CdSe QDSSCs using SWCNTs/TiO_2 nanocomposite photoanode at various intensities of solar illumination (from 0–100% sun) was also studied. Fig. 10(a) shows the *J–V* characteristics curves of the assembled CdSe QDSSCs for the 6 h dipping time assembly. It is seen that as the intensity of the incident light increases, the measured J_{sc} increases linearly due to increased electrons injection, as shown in Fig. 10(b). The approximately constant value of V_{oc} indicates the high sensitivity of CdSe QDSSCs based on SWCNTs/TiO_2 nanocomposite photoanode that was prepared by the DA method.

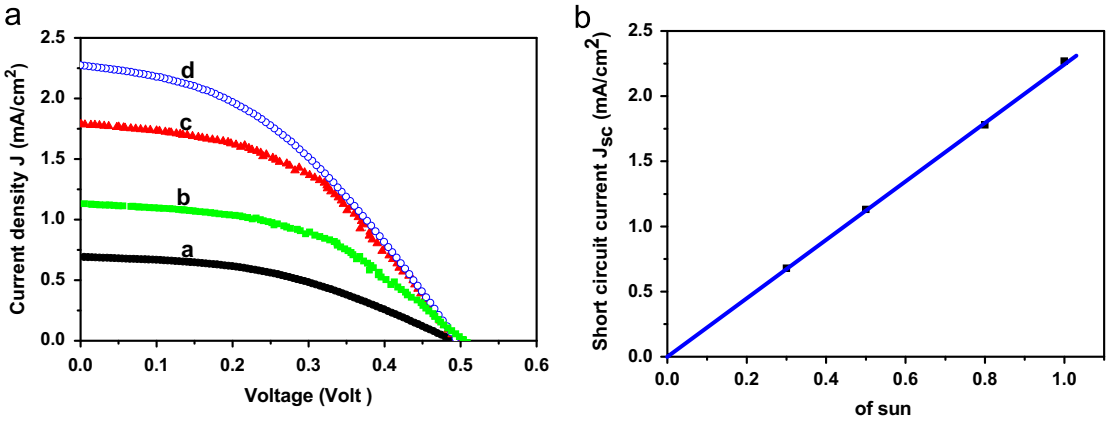

Fig. 10. (a): *J–V* characteristics curve of CdSe QDSSC using SWCNTs/TiO_2 nanocomposite photoanode for 6 h dipping time at a) 30%, b) 50%, c) 80%, and d) 100% of sun; (b) short circuit current density J_{sc} vs. the percentage of sun.

4. Conclusion

We have synthesized a paste of 0.2 wt% of single walled carbon nanotubes/Titania (0.2 wt% of SWCNTs/TiO_2) nanocomposite to fabricate quantum dots sensitized solar cells (QDSSCs) photoanodes. CdSe QDs of 4.52 nm in size were prepared and applied as a sensitizer for QDSSCs by direct adsorption (DA) technique onto 0.2 wt% SWCNTs/TiO_2 nanocomposite photoanode. A significant increase (~58%) in the energy conversion efficiency (η) was achieved in CdSe QDSSCs based on SWCNTs/TiO_2 nanocomposite as compared to others based on plain TiO_2 NPs under AM 1.5 simulated sunlight. The open circuit voltage (V_{oc}) is unchanged in both solar cells. The increase in η due to the increase in the photocurrent density (J) of the assembled QDSSCs is attributed to three factors: (i) the improvement in the absorption of the nanocomposite films due to increase loading of CdSe QDs on the film, (ii) rapid electron transport through the SWCNTs, offering fast interpaths due to the superior electrical conductivity of SWCNTs compared to the TiO_2 NPs, and (iii) the DA technique, used to deposit CdSe QDs onto SWCNTs/TiO_2 nanocomposite films, leads to pin the CdSe QDs to that of TiO_2 NPs without any barriers.

Acknowledgments

The authors wish to thank Taif University for the financial support. Quantum Optics Research Group (QORG) at Deanship of Scientific Research- Taif University is also thanked for their assistance during this work. The Egyptian STDF Grant ID 377 support is greatly appreciated.

References

[1] P.V. Kamat, J. Phys. Chem. C 112 (2008) 18737–18753.
[2] A. Badawi, N. Al-Hosiny, S. Abdallah, S. Negm, H. Talaat, Sol. Energy 88 (2013) 137–143.
[3] S. Kolahi, S. Farjami-Shayesteh, Y. Azizian-Kalandaragh, Mater. Sci. Semicond. Process. 14 (2011) 294–301.
[4] Z. El-Qahtani, A. Badawi, K. Easawi, N. Al-Hosiny, S. Abdallah, Mater. Sci. Semicond. Process. 20 (2014) 68–73.
[5] A. Badawi, K. Easawi, N. Al-Hosiny, S. Abdallah, Mater. Sci. Appl. 5 (2014) 27–32.
[6] Y. Xie, S.H. Yoo, C. Chen, S.O. Cho, Mater. Sci. Eng. B 177 (2012) 106–111.
[7] K. Tvrdy, P.A. Frantsuzov, P.V. Kamat, Proc. Natl. Acad. Sci. USA 108 (2011) 29–34.
[8] H. Chen, W. Li, H. Liu, L. Zhu, Electrochem. Commun. 13 (2011) 331–334.
[9] A. Salant, M. Shalom, I. Hod, A. Faust, A. Zaban, U. Banin, ACS Nano 4 (2010) 5962–5968.
[10] A. Kongkanand, K. Tvrdy, K. Takechi, M. Kuno, P.V. Kamat, J. Am. Chem. Soc. 130 (2008) 4007–4015.
[11] J. Kim, H. Choi, C. Nahm, J. Moon, C. Kim, S. Nam, D.-R. Jung, B. Park, J. Power Sources 196 (2011) 10526–10531.
[12] S. Emin, S.P. Singh, L. Han, N. Satoh, A. Islam, Sol. Energy 85 (2011) 1264–1282.
[13] A. Tubtimtae, K.-L. Wu, H.-Y. Tung, M.-W. Lee, G.J. Wang, Electrochem. Commun. 12 (2010) 1158–1160.
[14] S. Abdallah, N. Al-Hosiny, A. Badawi, J. Nanomater. 2012 (2012) 6.
[15] J. Jiao, Z.-J. Zhou, W.-H. Zhou, S.-X. Wu, Mater. Sci. Semicond. Process. 16 (2013) 435–440.
[16] F. Zhao, G. Tang, J. Zhang, Y. Lin, Electrochim. Acta 62 (2012) 396–401.
[17] A. Badawi, N. Al-Hosiny, S. Abdallah, H. Talaat, Mater. Sci.-Pol. 31 (2013) 6–13.
[18] D.R. Pernik, K. Tvrdy, J.G. Radich, P.V. Kamat, J. Phys. Chem. C 115 (2011) 13511–13519.
[19] X. Wang, H. Zhu, Y. Xu, H. Wang, Y. Tao, S. Hark, X. Xiao, Q. Li, ACS Nano 4 (2010) 3302–3308.
[20] S. Kitada, E. Kikuchi, A. Ohnob, S. Aramakib, S. Maenosono, Solid State Commun. 149 (2009) 1853–1855.
[21] B.-R. Hyun, Y.-W. Zhong, A.C. Bartnik, L. Sun, H.D. Abrun, F.W. Wise, J. D. Goodreau, J.R. Matthews, T.M. Leslie, N.F. Borrelli, ACS Nano 2 (2008) 2206–2212.
[22] Y. Liu, J. Wang, Thin Solid Films 518 (2010) e54–e56.
[23] P. Yu, K. Zhu, A.G. Norman, S. Ferrere, A.J. Frank, A.J. Nozik, J. Phys. Chem. B 110 (2006) 25451–25454.
[24] C.-C. Wang, L.-C. Chen, T.-C. Wang, J. Optoelectron. Adv. Mater. 11 (2009) 834–837.
[25] A. Tubtimtae, M.-W. Lee, G.-J. Wang, J. Power Sources 196 (2011) 6603–6608.
[26] I. Mora-Ser´o, S. Gim´enez, T. Moehl, F. Fabregat-Santiago, T. Lana-Villareal, R. G´omez, J. Bisquert, Nanotechnology (2008) 424007.
[27] S. Ruhle, M. Shalom, A. Zaban, ChemPhysChem 11 (2010) 2290–2304.
[28] N. Guijarro, T. Lana-Villarreal, I. Mora-Seró, J. Bisquert, R. Gómez, J. Phys. Chem. C 113 (2009) 4208–4214.
[29] J.H. Bang, P.V. Kamat, ACS Nano 3 (2009) 1467–1476.
[30] S. Giménez, I. Mora-Seró, L. Macor, N. Guijarro, T. Lana-Villarreal, R. Gómez, L.J. Diguna, Q. Shen, T. Toyoda, J. Bisquert, Nanotechnology 20 (2009) 295204.
[31] J. Yan, M.J. Uddin, T.J. Dickens, O.I. Okoli, Sol. Energy 96 (2013) 239–252.
[32] H. Chang, T.-J. Hsieh, T.-L. Chen, K.-D. Huang, C.-S. Jwo, S.-H. Chien, Mater. Trans. 50 (2009) 2879–2884.
[33] H. Anwar, A.E. George, I.G. Hill, Sol. Energy 88 (2013) 129–136.

[34] Y. Choi, Y. Kim, S.-G. Park, Y.-G. Kim, B.J. Sung, S.-Y. Jang, W. Kim, Org. Electron. 12 (2011) 2120–2125.
[35] J. Al-Osaimi, N. Alhosiny, A. Badawi, S. Abdallah, Int. J. Eng. Technol. IJET-IJENS 13 (2013) 77–79.
[36] E.R. Morales, N.R. Mathews, D. Reyes-Coronado, C.R. Magaña, D.R. Acosta, G. Alonso-Nunez, O.S. Martinez, X. Mathew, Sol. Energy 86 (2012) 1037–1044.
[37] J.Y. Ahn, J.H. Kim, K.J. Moon, J.H. Kim, C.S. Lee, M.Y. Kim, J.W. Kang, S.H. Kim, Sol. Energy 92 (2013) 41–46.
[38] G. Khurana, S. Sahoo, S.K. Barik, R.S. Katiyar, J. Alloys Compd. 578 (2013) 257–260.
[39] S.U. Lee, W.S. Choi, B. Hong, Sol. Energy Mater. Sol. Cells 94 (2010) 680–685.
[40] Z. Peining, A.S. Nair, Y. Shengyuan, P. Shengjie, N.K. Elumalai, S. Ramakrishna, J. Photochem. Photobiol. A: Chem. 231 (2012) 9–18.
[41] J. Yu, J. Fan, B. Cheng, J. Power Sources 196 (2011) 7891–7898.
[42] D.V. Talapin, S. Haubold, A.L. Rogach, A. Kornowski, M. Haase, H. Weller, J. Phys. Chem. B 105 (2001) 2260–2263.
[43] G. Syrrokostas, M. Giannouli, P. Yianoulis, Renew. Energy 34 (2009) 1759–1764.
[44] O. Madelung, Semiconductors: Data Handbook, 3rd ed. Springer-Verlag, Berlin, 2004.
[45] L. Brus, J. Phys. Chem. 90 (1986) 2555–2560.
[46] Parak, W.J., Manna, L., Simmel, F.C., Gerion, D., Alivisatos, P., Quantum Dots, in: Nanoparticles: From Theory to Application, G. Schmid (Ed.) Wiley-VCH Verlag GmbH & Co. KGaA, Weinheim, FRG, 2005, http://dx.doi.org/10.1002/3527602399.ch2.
[47] S. Ngamta, N. Boonprakob, N. Wetchakun, K. Ounnunkad, S. Phanichphant, B. Inceesungvorn, Mater. Lett. 105 (2013) 76–79.
[48] E.S. Lee, K.M. Lee, S.I. Yoon, Y.G. Ko, D.H. Shin, Curr. Appl. Phys. 13 (Suppl. 2) (2013) S26–S29.
[49] P.-C. Ma, N.A. Siddiqui, G. Marom, J.-K. Kim, Composites Part A 41 (2010) 1345–1367.
[50] K. Pomoni, M.V. Sofianou, T. Georgakopoulos, N. Boukos, C. Trapalis, J. Alloys Compd. 548 (2013) 194–200.